

## Theory of infrared absorption in silicon

K. Winer and M. Cardona

*Max-Planck-Institut für Festkörperforschung, Heisenbergstrasse 1, Postfach 80 06 65,  
D-7000 Stuttgart 80, Federal Republic of Germany*

(Received 1 December 1986)

A phenomenological theory of infrared (ir) absorption based on dipole moments derived from local charges produced by bond-length and bond-angle distortions is applied to calculate the ir absorption in crystalline (*c*-Si) and amorphous (*a*-Si) silicon. In *a*-Si, the first-order ir absorption is dominated by effective charges due to phonon-induced bond-angle distortions. In *c*-Si, the second-order ir absorption is best described by a phonon-modulated version of the same mechanism. A single value for the coupling constant in the dipole moments ( $e_0^* = 0.35e$ ) provides reasonably good agreement with the absolute experimental ir absorption spectrum of both *c*-Si and *a*-Si, demonstrating that the ir absorption in both cases can be well described by the same local charge-transfer mechanisms.

### I. INTRODUCTION

Symmetry selection rules and the conservation of crystal momentum lead to zero first-order infrared (ir) absorption in diamond-structure silicon (*c*-Si). The lack of long-range order in amorphous silicon (*a*-Si) relaxes these restrictions allowing all vibrational eigenmodes to contribute to the first-order ir absorption. The ir response of *c*-Si between zero and twice the Raman frequency ( $0 < \omega < 2\omega_R$ ) should be dominated by second-order (two-phonon) absorption.<sup>1</sup> Both the first- and second-order absorption processes can be described formally by the expansion of the crystal dipole moment in terms of the nuclear displacements; the term first order in the nuclear displacements corresponds to first-order absorption, etc. The crystal dipole moment is coupled to the nuclear displacements through effective charges, also known as dynamic or transverse charges. The matrix in the second-order term coupling the nuclear displacements to the crystal dipole moment contains seven distinct elements for the diamond structure,<sup>2</sup> and only five have been found to be essential to produce reasonable agreement with the experimental ir absorption spectrum of *c*-Si.<sup>3</sup>

Adjustment of the elements of the coupling matrix to fit the experimental ir absorption spectrum is perhaps the most straightforward method of interpreting the ir absorption of silicon. However, one can gain some insight into the absorption process itself by considering the local charge-transfer mechanisms that produce the dipole moments. We have recently described a theory of the first-order ir absorption in *a*-Si (Ref. 4) where the dipole moments are derived from local charges produced by phonon-induced bond-length and bond-angle distortions. Here we apply this theory, with no modifications, to calculate the absolute two-phonon ir absorption for *c*-Si. We briefly describe the local charge-transfer mechanisms and the derivation from them of the expressions for the first- and second-order ir absorption in Sec. II. We present the results of the calculation and discuss their significance in Sec. III. We find that the ir absorption in *a*-Si and *c*-Si

can be well described by the same local charge-transfer mechanisms. Finally, in Sec. IV, we make some predictions for the ir absorption of the crystalline B-8 ("BC8") Si polymorph.

### II. THEORY OF INFRARED ABSORPTION

We define two dipole moments<sup>4</sup> as illustrated in Fig. 1. One is due to the local charge transfer between bonds in adjacent bond pairs resulting from distortions of their bond lengths given by

$$\mathbf{P}_R = \sum_l \sum_j \sum_{i(>j)} [r_{li} - r_{lj}](\mathbf{r}_{li} - \mathbf{r}_{lj})/r_0, \quad (1)$$

where  $\mathbf{r}_{li} = r_{li} \hat{\mathbf{r}}_{li}$  is the bond vector between atoms *l* and *i*,  $r_0 = 2.35 \text{ \AA}$  is the equilibrium bond length in the diamond structure, and *i* and *j* are distinct, bonded nearest neighbors of atom *l*. This mechanism represents the transfer of negative charge from compressed to extended bonds.

The second dipole moment is due to the local charge transfer between atoms at either end of adjacent bonds resulting from distortions of the angle between the bonds given by

$$\mathbf{P}_\theta = \sum_l \sum_j \sum_{i(>j)} [\mathbf{r}_{li} \cdot \mathbf{r}_{lj} + \frac{1}{3} r_0^2](\mathbf{r}_{li} + \mathbf{r}_{lj})/r_0^2. \quad (2)$$

In order to obtain true dipole moments, Eqs. (1) and (2), and subsequent equivalent equations, must be multiplied by a coupling constant with the units of charge. These two expressions are translationally and rotationally invariant, orthogonal in the limit of constant bond length for each bond pair, and produce zero dipole moment when applied to the diamond structure, as they should. The terms in square brackets represent the charge transfer.

The absolute first-order ir absorption coefficient can be described by the following expression:<sup>5</sup>

$$\begin{aligned} \alpha(\omega) &= \omega \epsilon_2(\omega) / nc \\ &= (2\pi^2 / ncMV) \sum_v (e_v^*)^2 \delta(\omega - \omega_v), \end{aligned} \quad (3)$$

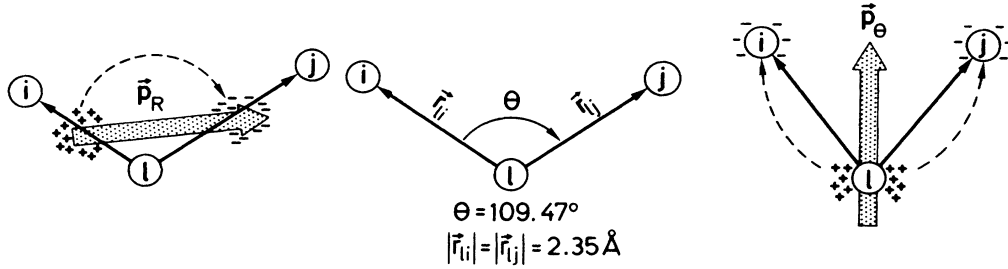


FIG. 1. Schematic representation of the local charge-transfer mechanisms used to describe the infrared absorption of *c*-Si and *a*-Si. Left, the transfer of negative charge from compressed to extended bonds. Right, the transfer of negative charge from the central atom to its adjacent neighbors for a “compressed” bond angle. Center, bond pair in the undistorted diamond structure. The dotted arrows depict the direction of charge transfer.

where  $\epsilon_2(\omega)$  is the imaginary part of the dielectric function,  $n$  the electronic (ir) index of refraction (taken to be 3.4 for both *a*-Si and *c*-Si),  $c$  the speed of light,  $M$  the mass of silicon, and  $V$  the volume of the unit cell. The sum is over all ir-allowed eigenmodes  $\nu$ , and  $e_\nu^*$  is the effective charge for mode  $\nu$  [ $(e_\nu^*)^2$  is usually a tensor. In an isotropic or cubic material, however, it reduces to a scalar]. We describe the effective charges in terms of the derivatives of Eqs. (1) and (2) (multiplied by coupling constants), each of which involves both a dynamic and a static charge-transfer component. The corresponding differentials are

$$\mu_1^\nu = \sum_l \sum_j \sum_{i(>j)} [\mathbf{u}_{li}^\nu \cdot \hat{\mathbf{r}}_{li} - \mathbf{u}_{lj}^\nu \cdot \hat{\mathbf{r}}_{lj}] (\mathbf{r}_{li} - \mathbf{r}_{lj}) / r_0, \quad (4)$$

$$\mu_1^\nu = \sum_l \sum_j \sum_{i(>j)} [r_{li} - r_{lj}] (\mathbf{u}_{li}^\nu - \mathbf{u}_{lj}^\nu) / r_0, \quad (5)$$

$$\mu_2^\nu = \sum_l \sum_j \sum_{i(>j)} [\mathbf{u}_{li}^\nu \cdot \mathbf{r}_{lj} + \mathbf{u}_{lj}^\nu \cdot \mathbf{r}_{li}] (\mathbf{r}_{li} + \mathbf{r}_{lj}) / r_0^2, \quad (6)$$

$$\mu_2^\nu = \sum_l \sum_j \sum_{i(>j)} [\mathbf{r}_{li} \cdot \mathbf{r}_{lj} + \frac{1}{3} r_0^2] (\mathbf{u}_{li}^\nu + \mathbf{u}_{lj}^\nu) / r_0^2, \quad (7)$$

where  $\mathbf{u}_{li}^\nu = \mathbf{u}_i^\nu - \mathbf{u}_l^\nu$ ,  $\mathbf{u}_i^\nu$  are the components of the eigenvector corresponding to the displacement of atom  $l$  for eigenmode  $\nu$ , and the prime designates the static charge-transfer mechanisms. The effective charge tensor corresponds to a dyadic built from the  $\mu$  vectors. We take the eigenmodes  $\mathbf{u}_i^\nu$  normalized to 1, i.e.,

$$\sum_l \mathbf{u}_l^\nu \cdot \mathbf{u}_l^\nu = 1, \quad (8)$$

where the summation is over all atoms in the unit cell.

A variant of Eq. (4) was first applied by Alben *et al.*<sup>6</sup> to the study of the ir absorption in *a*-Si. It corresponds to the local transfer of charge between bonds in adjacent bond pairs due to *phonon-induced* distortions in their bond lengths. We refer to this mechanism as dynamic stretching. The charges in Eqs. (5) and (7) are determined by the static distortions from tetrahedral bonding, which are in general small in *a*-Si. Equation (6) corresponds to the local transfer of charge between atoms at either end of adjacent bond pairs due to *phonon-induced* distortions in the angle between the bonds. We refer to this mechanism as dynamic bending.

We have shown<sup>4</sup> that only those terms that correspond

to dynamic charge transfer [Eqs. (4) and (6)] give appreciable contributions to the ir absorption in *a*-Si. Also, we have found that the vector sum of  $\mu_1^\nu$  and  $\mu_2^\nu$  provides the best agreement with the shape of the experimental ir absorption of *a*-Si as shown in Fig. 2. We can write the effective charges for each mode  $\nu$  as

$$e_\nu^* = e_0^* |\mu_1^\nu + \mu_2^\nu| / \sqrt{3}, \quad (9)$$

where  $e_0^*$  is a coupling constant equal to 0.35 electrons as determined by fitting the experimental spectrum with Eq. (3); the sign of the coupling constants is chosen to correspond to the transfer of negative charge due to the electronic repulsion caused by overlapping orbitals (see Fig. 1). There is no reason *a priori* why the magnitude of the coupling constants of  $\mathbf{P}_R$  and  $\mathbf{P}_\theta$  should be the same. However, as we will shortly show, equal charges are required for a good description of the absolute ir absorption of both *c*-Si and *a*-Si.

If we apply  $\mu_1^\nu$  and  $\mu_2^\nu$  to *c*-Si we get zero infrared absorption, as we must for the one-phonon absorption process. We can imagine the two-phonon ir absorption process in *c*-Si as follows. The first phonon displaces the atoms in the crystal. The phonon-induced lattice distortions that result lead to the local transfer of charges as discussed above. Because of the symmetry of the diamond structure, the resulting dipole moments will cancel exactly to give zero ir absorption. A second phonon can remove the dipole-moment-canceling symmetries by either moving the charges produced by the first phonon or inducing further charge transfer. The only restriction is that the total momentum of the two phonons must be equal to that of the incident photon ( $k \sim 0$ ) to obey momentum conservation rules. We treat this process by assuming that the charge transfer due to the two phonons can be described by the second derivative of  $\mathbf{P}_R$  and  $\mathbf{P}_\theta$ , which leads to the following expressions:

$$\rho_1^{\nu_1 \nu_2} = \sum_l \sum_j \sum_{i(>j)} [\mathbf{u}_{li}^{\nu_1} \cdot \hat{\mathbf{r}}_{li} - \mathbf{u}_{lj}^{\nu_1} \cdot \hat{\mathbf{r}}_{lj}] (\mathbf{u}_{li}^{\nu_2} - \mathbf{u}_{lj}^{\nu_2}) / r_0, \quad (10)$$

$$\rho_2^{\nu_1 \nu_2} = \sum_l \sum_j \sum_{i(>j)} [\mathbf{u}_{li}^{\nu_1} \cdot \mathbf{u}_{li}^{\nu_2} - \mathbf{u}_{lj}^{\nu_1} \cdot \mathbf{u}_{lj}^{\nu_2}] (\hat{\mathbf{r}}_{li} - \hat{\mathbf{r}}_{lj}) / r_0, \quad (11)$$

$$\rho_3^{\nu_1 \nu_2} = \sum_l \sum_j \sum_{i(>j)} [\mathbf{u}_{li}^{\nu_1} \cdot \hat{\mathbf{r}}_{lj} + \mathbf{u}_{lj}^{\nu_1} \cdot \hat{\mathbf{r}}_{li}] (\mathbf{u}_{li}^{\nu_2} + \mathbf{u}_{lj}^{\nu_2}) / r_0, \quad (12)$$

$$\rho_4^{v_1 v_2} = \sum_l \sum_j \sum_{i(>j)} [\mathbf{u}_{li}^{v_1} \cdot \mathbf{u}_{lj}^{v_2} + \mathbf{u}_{lj}^{v_1} \cdot \mathbf{u}_{li}^{v_2}] (\hat{\mathbf{r}}_{li} + \hat{\mathbf{r}}_{lj}) / r_0, \quad (13)$$

where we have recognized that only terms of second order in the displacements contribute to the two-phonon absorption. It can easily be shown that, because of the diamond structure symmetry, Eq. (11) is exactly zero, and Eqs. (10) and (12) are exactly equivalent, for any pair of modes  $v_1$  and  $v_2$ . We therefore restrict our attention to Eqs. (12) and (13), which are analogous to the static and dynamic charge-transfer mechanisms  $\mu_2'$  and  $\mu_2$ , respectively, described above and more fully in Ref. 4.

The absolute two-phonon ir absorption is then described by the following expression:<sup>10</sup>

$$\begin{aligned} \alpha(\omega) = & (\hbar\pi^2 / ncM^2V) \sum_{v_1} \sum_{v_2} [(\omega_{v_1} + \omega_{v_2}) / \omega_{v_1}\omega_{v_2}] \\ & \times [1 + \bar{n}(\omega_{v_1}) + \bar{n}(\omega_{v_2})] \\ & \times (e_{v_1 v_2}^*)^2 \delta(\omega - \omega_{v_1} - \omega_{v_2}), \end{aligned} \quad (14)$$

where  $\hbar$  is Planck's constant,  $\bar{n}(\omega_{v_1})$  the thermal average phonon occupation number for mode  $v_1$ , the sums are over all phonons with opposite momenta, and again the effective charges are given by

$$e_{v_1 v_2}^* = e_0^* |\rho_3^{v_1 v_2}| / \sqrt{3} \quad \text{or} \quad e_0^* |\rho_4^{v_1 v_2}| / \sqrt{3}. \quad (15)$$

We use Weber's adiabatic bond charge model<sup>11</sup> to calculate the eigenfrequencies  $\omega_v(\mathbf{k})$  and eigenvectors  $\mathbf{u}_v^*(\mathbf{k})$  of phonons with momentum vector  $\mathbf{k}$  on an  $11 \times 11 \times 11$  grid in the first Brillouin zone of the eight-atom diamond cubic unit cell of *c*-Si. Although random  $\mathbf{k}$  vectors or the tetrahedron method would provide more accurate results, we choose a regular grid for computational convenience. The two-phonon density of states we obtain is in good quantitative agreement with (although a bit noisier than) that obtained by the more accurate methods. We approximate the delta function in Eq. (14) by a Gaussian with a full width at half maximum of  $5.3 \text{ cm}^{-1}$ . The calculation is performed for  $T=290 \text{ K}$ , where the main effect of the frequency difference terms<sup>10</sup> we have neglected in Eq. (14) is to slightly enhance the low-frequency absorption.

### III. RESULTS AND DISCUSSION

The results of the two-phonon ir absorption calculation are shown in Fig. 3 along with the calculated two-phonon density of states and the experimental ir absorption of *c*-Si (Ref. 12). We note that the two-phonon density of states, except at the frequency extremes, provides a rough approximation to the shape of the ir absorption spectrum. The main effect of the matrix elements, i.e., the effective charges, should be to suppress the high- and low-frequency features with respect to the mid-frequency ones.

There are two main sources of error, other than the effective charge ansatz, that might account for any discrepancies in the present calculation. Although the Weber bond charge model provides a reasonably good fit to the experimental phonon dispersion curves of *c*-Si,<sup>11</sup> deviations along the *L* and *K* directions are as high as five percent. These directions contribute particularly strongly to the infrared absorption.<sup>3</sup> One can get some idea of the discrepancies involved due to the inadequacy of the Weber model by comparing the peak positions in the two-phonon density of states with those in the experimental ir absorption spectrum. The matrix elements, in the form of the effective charges, modify the density of states in a smooth manner, so that major peaks in the density of states should remain identifiable in the experimental ir absorption. One can see that the agreement in the frequencies of most, but not all, of the peaks is within a few percent or so. We thus believe that inaccuracies in Weber's model

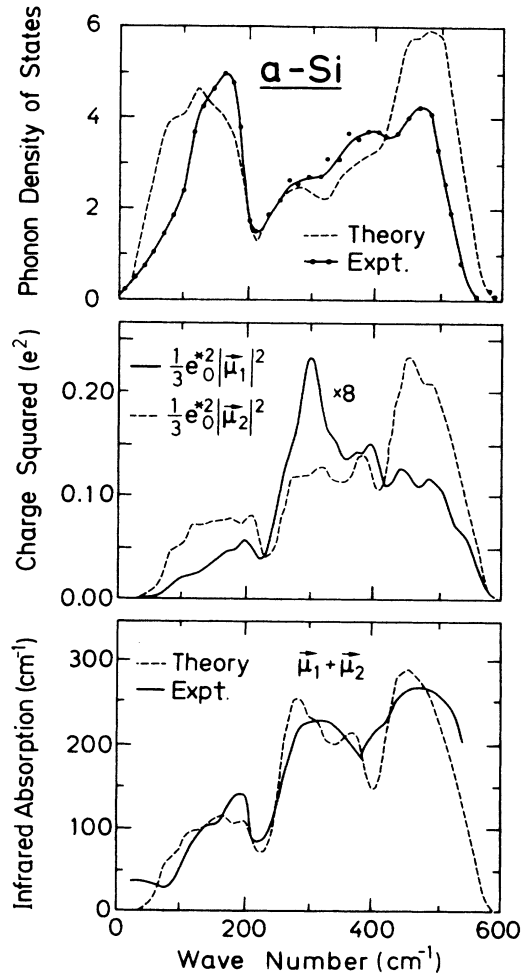


FIG. 2. Vibrational properties of *a*-Si. Top, phonon density of states calculated for a 216-atom continuous distorted network (CDN) model of *a*-Si using Weber's bond charge interactions (Ref. 7) compared to the results of neutron scattering (Ref. 8). Middle, comparison of the contributions for the dynamic stretching  $\mu_1$  and bending  $\mu_2$  mechanisms for the same 216-atom CDN model (Ref. 4). Bottom, absolute ir absorption of *a*-Si calculated using the vector sum of the stretching and bending mechanisms with a coupling constant ( $e_0^*$ ) of  $0.35e$ . The calculation is compared to the measured ir absorption of *a*-Si (Ref. 9).

are the major source of error as far as peak positions are concerned.

A second source of error arises from the neglect of higher-order absorption processes. We expect that the most serious consequence of this neglect might be a slight underestimation of the ir absorption at higher frequencies. It can readily be seen in Fig. 3 that the underestimation, if any, is small.

The ir absorption spectra derived from  $\rho_3$  and  $\rho_4$  are quite different from each other in terms of both shape and intensity, as can be seen in Fig. 3. This is also the case for

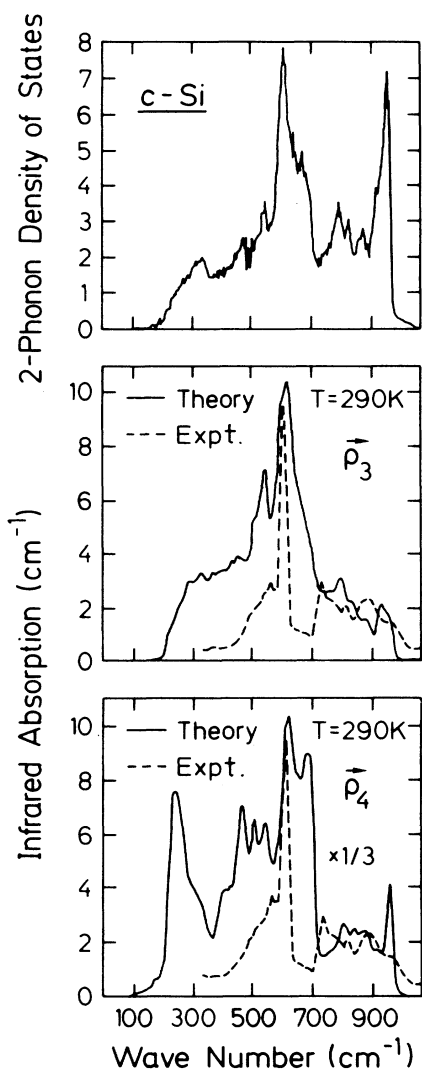


FIG. 3. Two-phonon vibrational properties of *c*-Si. Top, two-phonon density of states calculated for an eight-atom cubic unit cell of *c*-Si using Weber's adiabatic bond charge interactions (Ref. 11) on an  $11 \times 11 \times 11$  point grid in the first Brillouin zone. Middle, the absolute two-phonon ir absorption of *c*-Si calculated using mechanism  $\rho_3$  and Eq. (14). Bottom, the same calculated using mechanism  $\rho_4$  and Eq. (14). The coupling constant is taken to be  $e_0^* = 0.35e$  for both calculated spectra. The results are compared to the experimental ir absorption spectrum of *c*-Si (Ref. 12).

the dynamic stretching  $\mu_1$  and bending  $\mu_2$  mechanisms applied here to *a*-Si (see Fig. 2). Perhaps most pertinent to the present results is the fact that the static stretching and bending mechanisms  $\mu'_1$  and  $\mu'_2$ , respectively, provide almost the same results when applied to the *a*-Si model: a much reduced intensity compared to the dynamic mechanisms and a shape similar to that of the phonon density of states.<sup>4</sup> The large differences in the spectral distributions and intensities of  $\mu_1$  compared to  $\mu_2$  in the amorphous case are partially due to the difference in the magnitude of the average bond-length and bond-angle distortions found in the amorphous model structure, 2% and 10%, respectively.<sup>7</sup>

Alben *et al.*<sup>13</sup> have shown that the intensity of the ir absorption calculated from  $\mu_1$  should scale roughly as the square of the distortion from tetrahedral symmetry. They have also shown that in the case of exact tetrahedral bonding and central forces, the infrared absorption from  $\mu_1$  should be dominated by mid-frequency components; the intensity of the absorption at high or low frequencies should be of fourth order in the distortions. This is certainly the case for the contribution of  $\mu_1$  to the ir absorption in *a*-Si as shown in Fig. 2, despite the  $\sim 2\%$  average deviation from the diamond-structure bond length and the inclusion of noncentral forces. Although the ir absorption calculated for  $\mu_2$  should also roughly scale as the square of the distortion from tetrahedral symmetry, it should not be dominated by mid-frequency contributions. Because of the plus sign in Eq. (6), the charge transfer remains first order in the phonon-induced bond-angle distortions for *all* eigenmodes. This, coupled with the much larger average angular distortions ( $\sim 10\%$ ) in the model structure, provides the significant contribution to the calculated ir absorption at low and high frequencies that is necessary to obtain good agreement with experiment in *a*-Si.

The behavior of the two-phonon ir absorption of *c*-Si can be partially understood in this light. The low- and high-frequency peaks in the two-phonon density of states in *c*-Si are composed essentially of modes with significant TA-TA (bend-bend) and TO-TO (stretch-stretch) character, respectively. We expect that the distortions away from tetrahedral bonding due to the two-phonon displacements for all combinations of eigenmodes (both bending and stretching) will in general be small. Therefore the ir absorption spectrum derived from  $\rho_1$  and  $\rho_3$ , the second-order (phonon-modulated) versions of the first-order static stretching and bending mechanisms  $\mu'_1$  and  $\mu'_2$ , respectively, should be relatively weak with a shape similar to that of the two-phonon density of states. We have already made note of the fact that the latter is a reasonable approximation to the experimental ir absorption spectrum except at low and high frequencies. The reduced contribution to the ir absorption derived from  $\rho_1$  and  $\rho_3$  at high frequencies due to the inverse frequency dependence should provide a good approximation to the shape of the ir absorption spectrum in *c*-Si.

At the same time, we expect that the ir absorption due to  $\rho_4$ , the second-order analog of the first-order dynamic bending mechanism  $\mu_2$ , should have significant contributions at both high and low frequencies. This is indeed the case as shown in Fig. 3; however, the "wings" in the  $\rho_4$

spectrum of *c*-Si are considerably reduced compared to those in the analogous  $\mu_2$  spectrum of *a*-Si due both to the inverse frequency dependence of the two-phonon ir absorption, which reduces the intensity of the high-frequency components, and to the lack of large (phonon-induced) deviations from tetrahedral bonding in *c*-Si.

Not only is the ir absorption derived from  $\rho_3$  in good qualitative agreement with the shape of the experimental spectrum, but by using the same coupling constant that gives the best fit to the absolute ir absorption spectrum of *a*-Si ( $e_0^* = 0.35e$ ), we also obtain excellent quantitative agreement with the absolute ir absorption of *c*-Si at the frequency of maximum absorption.

We note that the effective charge at the absorption maximum (at  $450 \text{ cm}^{-1}$ ) in *a*-Si has a value of  $0.46e$ , which is in excellent agreement with the value of the transverse charge calculated by Shen and Cardona<sup>14</sup> of  $0.51e$ . They used the integrated experimental ir absorption (*f*-sum rule) of *a*-Si to estimate the effective charge assuming a chemically ordered structure like GaAs. They suggested that the charges might be localized on dangling bonds at the surfaces of voids. The excellent agreement with the absolute ir absorption of *a*-Si obtained with the local charge-transfer ansatz, however, indicates that simple geometric distortions in the bulk are sufficient to account for the relatively large dynamical charges in *a*-Si. Further support for this view derives from the good agreement with the absolute strength of the two-phonon ir absorption of *c*-Si using the same coupling constant and same local charge-transfer ansatz as in *a*-Si. Certainly the effective charges in *c*-Si ( $e_{v_1+v_2}^* = 0.72e$  at  $1000 \text{ cm}^{-1}$ ) do not arise from dangling bonds at voids or from any other defect-related mechanisms. Although the effective charge in the crystal cannot be directly compared with that derived for *a*-Si, the fact that the coupling constant that produces good quantitative agreement with experiment in both *c*-Si and *a*-Si is essentially the same demonstrates that the local transfer of charges due to *phonon-induced* deviations from tetrahedral bonding is the dominant dipole-producing mechanism in both phases of silicon. We note, however, that the addition of  $\rho_1$  to  $\rho_3$  (the two contributions are equivalent) would decrease the coupling constant in *c*-Si by a factor of 2.

The two-phonon ir absorption derived from  $\rho_4$  is in poor agreement with experiment. We have investigated the interference behavior of  $\rho_3$  and  $\rho_4$  to see if some combination of these two mechanisms might improve the agreement. The interference is generally small ( $\sim 15\%$  of the absorption due to  $\rho_3$  alone, see Fig. 3) with roughly equal numbers of sharp positive and negative peaks distributed at random over the entire frequency range. We find therefore that the vector sum or difference of  $\rho_3$  and  $\rho_4$  also provide a poor approximation to the experimental ir absorption spectrum.

We do not understand why the calculated ir absorption derived from a simple combination of the phonon-induced dipoles (vector sum) should produce good agreement with experiment in the amorphous phase but not in crystalline silicon. We note, however, that in a microscopic theory the coupling constants would be related to the spectrum of electronic excitations, which is considerably different in

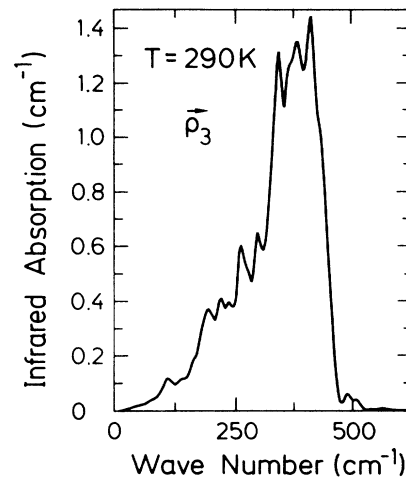


FIG. 4. Two-phonon absolute ir absorption calculated using mechanism  $\rho_3$  ( $e_0^* = 0.35e$ ) and the frequency difference analog of Eq. (14) (Ref. 10) for  $T = 290 \text{ K}$ .

amorphous and crystalline silicon. Difficulties in transferring coupling constants from one semiconductor to another have been reported earlier.<sup>15</sup>

For the sake of completeness we show in Fig. 4 the two-phonon frequency difference ir absorption spectrum of *c*-Si at 290 K calculated with our  $\rho_3$  ansatz ( $e_0^* = 0.35e$ ). The ir absorption due to this term vanishes at zero temperature and is small at room temperature. Absorption measurements at several temperatures should help to separate it from the frequency sum spectrum discussed above. Such a procedure has not yet been carried out.

#### IV. PREDICTIONS FOR BC8 Si

Although few experimental investigations of the properties of BC8 Si have been made since its discovery more than 20 years ago,<sup>16,17</sup> several theoretical studies of this high-density silicon polymorph have been undertaken<sup>18,19</sup> so that the structural and vibrational properties of the ideal BC8 Si crystal are well known.<sup>20</sup>

The structure of BC8 Si is characterized by geometric distortions similar in magnitude to those in *a*-Si (Ref. 20) and its symmetry allows only two ir active modes of vibration. In Table I we give the absolute integrated first-order ir absorption of BC8 Si determined by using the ir absorption expression in Eq. (3) and by applying the dynamic stretching  $\mu_1$  and bending  $\mu_2$  mechanisms to the vibrational eigenmodes calculated with Weber's bond charge interactions.<sup>11,20</sup>

As in *a*-Si, the spectral distribution of the ir absorption in BC8 Si calculated from  $\mu_1$  is completely different from that calculated from  $\mu_2$ . The dominant high-frequency contribution for the stretching mechanism is consistent with the dominant stretching character of the high-frequency (TO) modes. Similarly, the dominant contribution from the bending mechanism is at low frequency, where the modes (TA) have a predominantly bending character.

TABLE I. Absolute integrated first-order ir absorption predicted for BC8 Si based on eigenmodes calculated using Weber's adiabatic bond charge model (Refs. 11 and 20) and Eq. (3) in the text ( $e_0^* = 0.35e$ ). The integrated value is given separately for both of the well-separated ir-active modes. Note that both of the ir-active modes are threefold degenerate. For comparison, the total integrated ir absorption in *a*-Si is  $7.3 \times 10^4 \text{ cm}^{-2}$  (Ref. 14).

Mechanism	$\int \alpha(\omega) d\omega \text{ (cm}^{-2}\text{)}$	
	$\omega = 220 \text{ cm}^{-1}$	$\omega = 415 \text{ cm}^{-1}$
$\mu_1$	$1.3 \times 10^3$	$8.2 \times 10^4$
$\mu_2$	$1.8 \times 10^5$	$2.0 \times 10^4$
$\mu_1 + \mu_2$	$2.0 \times 10^5$	$2.0 \times 10^4$
$\mu_1 - \mu_2$	$2.3 \times 10^5$	$1.6 \times 10^5$

The fact that the predicted absolute integrated ir absorption is larger than that of *a*-Si (Ref. 14) is due to the symmetry of the BC8 Si structure. In *a*-Si the resultant dipole moment for the six bond pairs associated with each atom will be arranged more or less at random within the constraints of tetrahedral coordination. Such a distribution leads to an averaging of the dipole moments over many nonequivalent directions and reduces the strength of the absorption through destructive interference. In crystalline BC8 Si, the dipole moments can interfere constructively, leading to a larger integrated first-order ir absorption than in *a*-Si even though the average geometric distortions are essentially equivalent.

We have calculated the LO-TO splitting for both of the ir-active modes using the following expression:<sup>5</sup>

$$\omega_{\text{LO}} - \omega_{\text{TO}} \approx c \int \alpha(\omega) d\omega / \pi n \omega, \quad (16)$$

and the results are presented in Table II. The splitting is small except for the low-frequency bending contribution, whose absolute ir absorption dominates the calculated spectrum. For comparison, the LO-TO splitting in GaAs is about  $20 \text{ cm}^{-1}$ .<sup>21</sup>

The ir absorption of BC8 Si has yet to be measured ex-

TABLE II. LO-TO splitting calculated for the two ir-active modes of BC8 Si using the two dynamic mechanisms described in the text ( $e_0^* = 0.35e$ ). For comparison, the splitting in GaAs is about  $20 \text{ cm}^{-1}$  (Ref. 21).

Mechanism	$\omega_{\text{LO}} - \omega_{\text{TO}} \text{ (cm}^{-1}\text{)}$	
	$\omega = 220 \text{ cm}^{-1}$	$\omega = 415 \text{ cm}^{-1}$
$\mu_1$	0.1	2.9
$\mu_2$	12.2	0.7

perimentally due to many complicating factors, the most troublesome of which is the lack of large samples. Because of the simplicity of the expected ir absorption in BC8 Si, the measurement of its ir absorption would provide a severe test of this theory.

## V. CONCLUDING REMARKS

It is satisfying that the ir absorption in silicon can be described by local (short-range) charge-transfer mechanisms without the need to consider correlations beyond first nearest neighbors. This allows the treatment of the ir absorption of both crystalline (two-phonon) and amorphous (one-phonon) silicon with the same local charge-transfer ansatz. We expect that this theory, with little or no modification, can provide a reasonable description of the absolute ir absorption of the crystalline and amorphous phases of other tetrahedral semiconductors.

*Note added in proof:* We have recently observed the ir absorption spectrum due to two differences in *c*-Si. It has a shape in agreement with Fig. 4, but its maximum is an order of magnitude smaller.

## ACKNOWLEDGMENT

One of us (K.W.) thanks the Alexander von Humboldt-Stiftung (Bonn, Germany) for continuing support.

<sup>1</sup>M. Lax and E. Burstien, *Phys. Rev.* **97**, 39 (1955).

<sup>2</sup>R. Wehner, *Phys. Status Solidi* **17**, K179 (1966).

<sup>3</sup>W. Kress, H. Borik, and R. K. Wehner, *Phys. Status Solidi* **29**, 133 (1968).

<sup>4</sup>K. Winer and M. Cardona, *Solid State Commun.* **60**, 327 (1986). We note that Eq. (7) in this reference is incorrect and should be replaced by Eq. (3) in the present text.

<sup>5</sup>M. Cardona, in *Light Scattering in Solids II*, edited by M. Cardona and G. Güntherodt (Springer-Verlag, New York, 1982), p. 58.

<sup>6</sup>R. Alben, J. E. Smith, Jr., M. H. Brodsky, and D. Weaire, *Phys. Rev. Lett.* **30**, 1141 (1973).

<sup>7</sup>K. Winer, *Phys. Rev. B* **35**, 2366 (1987).

<sup>8</sup>W. A. Kamatikahara, H. R. Shanks, J. F. McClelland, U. Buchenau, F. Gompf, and L. Pintchovious, *Phys. Rev. Lett.* **52**, 644 (1984).

<sup>9</sup>S. C. Shen, C. J. Fang, M. Cardona, and L. Genzel, *Phys. Rev.*

*B* **22**, 2913 (1980).

<sup>10</sup>B. Szigeti, *Proc. R. Soc. London* **258**, 377 (1960).

<sup>11</sup>W. Weber, *Phys. Rev. B* **15**, 4789 (1977).

<sup>12</sup>F. A. Johnson, *Progress in Semiconductors* (Temple, London, 1965), Vol. 9, p. 178.

<sup>13</sup>R. Alben, D. Weaire, M. F. Thorpe, and M. H. Brodsky, *Phys. Rev. B* **11**, 2271 (1975).

<sup>14</sup>S. C. Shen and M. Cardona, *Phys. Rev. B* **23**, 5322 (1980). Exact agreement with the experimentally derived effective charge is in fact required because the formalism used by Shen and Cardona and in the present study is the same. The variations in the shape of the calculated and experimental ir absorption spectra account for the discrepancy in the effective charge values.

<sup>15</sup>S. Go, H. Bilz, and M. Cardona, *Phys. Rev. Lett.* **34**, 580 (1974).

<sup>16</sup>J. S. Kasper and R. H. Wentorf, Jr., *Science* (Washington)

- 139, 338 (1963).
- <sup>17</sup>J. S. Kasper and S. M. Richards, *Acta Cryst.* **17**, 752 (1964).
- <sup>18</sup>J. D. Joannopoulos and M. L. Cohen, *Phys. Rev. B* **7**, 2644 (1973).
- <sup>19</sup>A. Goldberg, M. El-Batanouny, and F. Wooten, *Phys. Rev. B* **26**, 6661 (1982).
- <sup>20</sup>K. Winer and F. Wooten, *Phys. Status Solidi B* **136**, 519 (1986).
- <sup>21</sup>H. R. Chandrasekhar and A. K. Ramdas, *Phys. Rev. B* **21**, 1511 (1980).